The preprint version of the article: S. R. Nekoo and A. Ollero, "Equivalent Vertical Dynamics of Flapping-Wing Flying Robot in Regulation Control: Displacement Transmissibility Ratio," 2023 International Conference on Unmanned Aircraft Systems (ICUAS), Warsaw, Poland, 2023, pp. 1301-1307, doi: 10.1109/ICUAS57906.2023.10156157.

Equivalent Vertical Dynamics of Flapping-Wing Flying Robot in Regulation Control: Displacement Transmissibility Ratio

Saeed Rafee Nekoo and Anibal Ollero
GRVC Robotics Lab., Departamento de Ingeniería de Sistemas y Automática
Escuela Técnica Superior de Ingeniería, Universidad de Sevilla, Seville, Spain
Emails: saerafee@yahoo.com, aollero@us.es
ORCID: 0000-0003-1396-5082, 0000-0003-2155-2472

***Abstract*—This paper presents an equivalent dynamic model for vertical regulation control of a flapping-wing flying robot. The model is presented based on the data of a series of flight experiments for an available platform. The system shows oscillations in motion in all experiments with an approximate frequency between $[3.5, 4.5]$(Hz), changing within a limited range. The behavior of the equivalent model represents a system with base excitation. The displacement transmissibility ratio (TR) is found for the model to investigate the oscillatory behavior in the system during the flight. Reduction of the oscillations through the transmissibility ratio will decrease the uncertainty in flight and consequently, that could increase the success rate of perching on a branch (now it has a $10-15$(cm) uncertain periodic motion); perching needs precision on the last meter approaching phase. An analytical expression for TR is presented which is used for parameter selection, tuning, and selection of the flapping frequency, as the base excitation source. The study shows that the robot works in a proper zone of the frequency ratio, and also, the sensitivity of the TR is high concerning the changes in the stiffness constant.**

Keywords*—Dynamics, Flapping-wing, Robot, Equivalent, Transmissibility ratio.

I. INTRODUCTION

The transmissibility ratio (TR) in mechanical vibration is a fundamental design characteristic to avoid the negative effect of an applied periodic load on the structure of a system. The TR was presented in analytical expressions for second-order standard mass-spring systems with and without damping components [1-4]. One of the main advantages of finding an analytical expression for TR is to see the behavior of the system with variation of damping and frequency ratio which indirectly defines stiffness and damping constant; the TR also presents a safe range for the frequency of oscillation of the base excitation over natural frequency, so-called "frequency ratio."

The transmissibility ratio can be considered for both force and displacement cases [5]. Wang et al. presented a quasi-zero stiffness vibration isolator for a two-degree-of-freedom (DoF) system with base excitation [6]. It was reported that the isolator design outperformed the passive controller in diminishing the transferred vibrations. The different TR values could be found with different damping ratios [7].

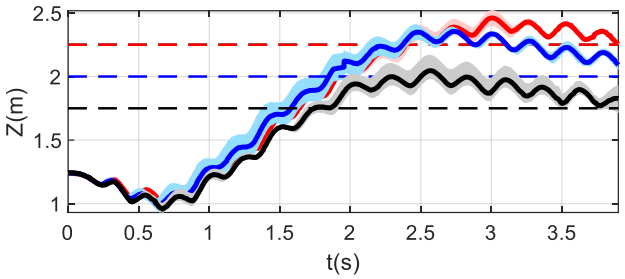

Fig. 1. Regulation and behavior of the flapping-wing robot in vertical motion for a series of experiments [8].

Ye and Ji investigated the vibration isolation problem for a truss-spring-based structure [9]. The absolute relation of the displacement transmissibility ratio was found to assess the performance of the isolator. A ring vibration isolator was also studied using a nonlinear energy sink [10]. In designing the vibration isolator, the transmissibility ratio was an important index for the evaluation of the design and isolator [5, 7, 9-12].

The flapping-wing flying robot (FWFR) is a challenging platform in aerial robotics [13-20]. Mou et al. presented active disturbance rejection for a flapping wing system subjected to internal and external disturbance [21]. Some of the challenges could be listed as different behavior in the downstroke and upstroke motion of the wings which makes the modeling a difficult task, the weight of the robot that could be kept at a minimum rate, and oscillation of the wings in a periodic way. A flapping-wing mechanism exerts periodic oscillatory lift force which is produced by wings. The actuation could be generated by direct current (DC) or brushless motors plus a crank-and-gear mechanism [14, 18, 19]; it could be produced by servo motors [22], clap-and-fling mechanism [23], or by elastic actuation based on an inverted-cam mechanical mechanism [24]. Regardless of actuation type, the periodic transferred base-excitation force should be controlled [25]. The periodic flapping reveals transient/steady-state oscillations in the flight pattern, especially in the height (vertical) control [8, 18], please see Fig. 1. These oscillations on the vertical trajectory impose an uncertain characteristic with an approximate amplitude of 15(cm) [8]. The closed-loop control was implemented for perching on a branch using an active leg to compensate for the oscillation in flight [8].

The preprint version of the article: S. R. Nekoo and A. Ollero, "Equivalent Vertical Dynamics of Flapping-Wing Flying Robot in Regulation Control: Displacement Transmissibility Ratio," 2023 International Conference on Unmanned Aircraft Systems (ICUAS), Warsaw, Poland, 2023, pp. 1301-1307, doi: 10.1109/ICUAS57906.2023.10156157.

Despite the success in perching and closed-loop controlled flight, it would be helpful to reduce the oscillatory behavior of the FWFR: it could increase the flight precision, add more robustness to the perching success rate, and increase the quality of the recorded data by cameras in case of using the system for the inspection missions [14, 26-31]. Sensor fusion was also addressed to gather data for the experiments for flapping flight [32].

To reduce the oscillations, the source of excitation and the model of the system are demanded to analyze the phenomena. The flapping-wing dynamic is complex and requires experimentation and computational fluid dynamics (CFD) analysis to develop the transient behavior of the system [33-37]. Ruiz et al. presented a reduced-order Volterra model for a flapping-wing flying robot system [33]. Sanchez-Laulhe et al. presented a simplified model for forward flight transition for FWFR [34]. Au et al. researched CFD analysis and dynamics of flapping wing small UAVs to study the effect of corrugation on aerodynamic performance [35]. Aerodynamic analysis and flight tests were performed for a bat-inspired tailless flapping wing [36]. Xiaowu et al. used CFD analysis for validation of the model, comparing the force and inertial results with experimental data of the flapping-wing system [38].

Despite various valuable research on the dynamics of FWFR and CFD analysis, a study of transmissibility ratio on the numerical model or analytical nonlinear systems is still a challenge because the proposed dynamics are too complex for finding an analytical answer to the TR. The objective of this work is to find an equivalent dynamic equation of motion of the FWFR system to first, find the TR and later study the behavior of the flapping-wing system in different ranges of flapping frequency, which in other words, denotes the excitation of the base. The possibility of reducing the displacement transmissibility ratio motivates us to find these crucial characteristics and improve the precision of the flight (with oscillations with lower amplitude) and perch on a branch easier. The equivalent dynamic is found by modeling the vertical motion of the FWFR based on the data received from a series of flight experiments. The flapping wing robot is limited to the actuation of the system with a limited range of frequency. It is important to define the base excitation in that range in which the TR is low and hence it transfers the minimum periodic excitation to the body of the ornithopter.

The main contributions of this work are to:

1) Deliver an equivalent model for vertical controlled motion of the flapping-wing flying robot based on the data of the experiment.

2) Find an analytical expression for the displacement transmissibility ratio for the equivalent FWFR model.

The rest of the work is organized as follows. Section II describes the problem statement. Section III presents the equivalent dynamic modeling. Section IV presents numerical analysis and presents the data for different ranges of damping and frequency ratios. Section V studies the parameter selection for the available ornithopter to find the proper flapping frequency and the corresponding TR for the system. Finally, conclusions are reported in Section VI.

II. Problem Statement

The motion of the flapping-wing robot is subjected to vertical oscillations caused by the flapping action. The flapping provides the lift force to move the robot up and keep it steady (around a vertical set-point) in flight; a reduction in flapping frequency also regulates the flight to lower heights. One of the advantages of flapping-wing systems is the ability to switch between the flapping and gliding modes. Of course, the gliding mode needs a favorable wind to maintain the elevation of the robot by the lift force. This will significantly reduce energy consumption and ideally, gliding could be considered as flapping limits. Going back to the fact that flapping mode is an inseparable part of the FWFR, it is crucial to model and study the effect of flapping on flight and its consequent generated oscillations.

Theoretically, the frequency of flapping could vary in any range; an example is a finite-element-based study that considered the flapping range between $[0,6](\mathrm{Hz})$, reported in [33]. In practice and reality, very low-frequency flapping might not even provide the possibility of flight. In experimentation and real flights, the operational flapping frequency was limited to $[3.5,4.5](\mathrm{Hz})$ [18]. The vertical regulation of the robot in a series of experiments is shown in Fig. 1. The amplitude of the oscillations is approximately between $[0.1,0.15](\mathrm{m})$ [8]. The experiments of flights were done for three different set-points of $1.75,2,2.25(\mathrm{m})$ height and the robot was launched from $1.25(\mathrm{m})$ height with an initial speed of $4(\mathrm{m/s})$.

The elevation model of the flapping robot could be presented as an equivalent mass-spring-damper one-degree-of-freedom system with base excitation, shown in Fig. 2. The motion of the tail controls the pitch angle of the robot and the effect of that on the vertical motion is neglected (in transient response) for the sake of simplicity. In the control loop of the flapping-wing robot, the frequency of flapping defines the elevation of the system. The dynamics of the system are also valid while the robot flies forward with a speed of $[2,6]\left(\frac{\mathrm{m}}{\mathrm{s}}\right)$, which was usually obtained in experiments.

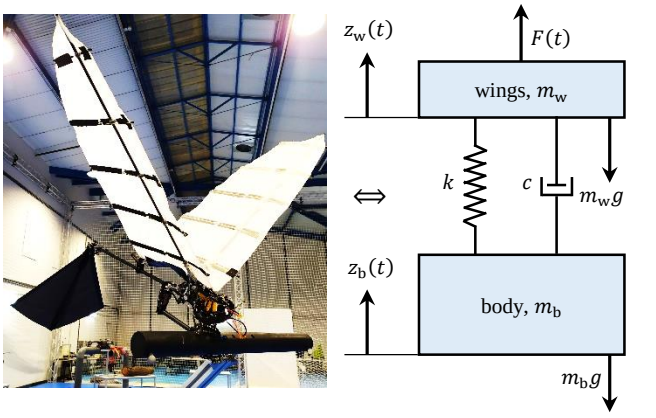

Fig. 2. The configuration of the flapping-wing robot and presentation of the equivalent dynamic with base excitation.

The preprint version of the article: S. R. Nekoo and A. Ollero, "Equivalent Vertical Dynamics of Flapping-Wing Flying Robot in Regulation Control: Displacement Transmissibility Ratio," 2023 International Conference on Unmanned Aircraft Systems (ICUAS), Warsaw, Poland, 2023, pp. 1301-1307, doi: 10.1109/ICUAS57906.2023.10156157.

III. Equivalent Dynamic Modeling

This section aims to find the displacement transmissibility ratio of the flapping-wing robot. Then the reduction of transmission ratio could be investigated clearer by the selection of proper damping and stiffness constants, or in other words, parameters of the system. Considering the mentioned assumptions in Section II, and observations from experiments, the following model is presented:

$$\begin{aligned} m_\mathrm{b}\ddot{z}_\mathrm{b}(t) + c\dot{z}_\mathrm{b}(t) + kz_\mathrm{b}(t) + (m_\mathrm{b}+m_\mathrm{w})g \\ = m_\mathrm{w}\ddot{z}_\mathrm{w}(t) + c\dot{z}_\mathrm{w}(t) + kz_\mathrm{w}(t) \\ + \bar{F}(t), \end{aligned} \tag{1}$$

where m_b and $m_\mathrm{w}(\mathrm{kg})$ are mass of base and wings respectively, $c(\mathrm{Ns/m})$ is damping coefficient, $k(\mathrm{N/m})$ is stiffness coefficient, $z_\mathrm{b}(t) \in \mathbb{R}$ is a generalized coordinate of the system and $z_\mathrm{w}(t) \in \mathbb{R}$ is the excitation of the base, which in this case, is the generated oscillatory motion caused by flapping, and $g = 9.81(\mathrm{m/s^2})$ is the gravity constant. $\bar{F}(t) \in \mathbb{R}$ is an input lift force produced by flapping that moves the robot higher or lower than the steady-state flight height based on the maximum and minimum range of flapping frequency.

The excitation of the base is defined as

$$\begin{aligned} z_\mathrm{w}(t) &= z_0 \sin(\omega(t)t), \\ \dot{z}_\mathrm{w}(t) &= z_0\{\omega(t) + \dot{\omega}(t)t\}\cos(\omega(t)t), \\ \ddot{z}_\mathrm{w}(t) &= z_0[\{2\dot{\omega}(t) + \ddot{\omega}(t)t\}\cos(\omega(t)t) \\ &\quad - \{\omega(t) + \dot{\omega}(t)t\}^2 \sin(\omega(t)t)], \end{aligned} \tag{2}$$

where $z_0(\mathrm{m})$ is the amplitude of the base excitation and $\omega(t) \in \mathbb{R}$ is the frequency of the flapping wing in $\left(\frac{\mathrm{rad}}{\mathrm{s}}\right)$. Substitution of (2) into (1) results in

$$\begin{aligned} m_\mathrm{b}\ddot{z}_\mathrm{b}(t) + c\dot{z}_\mathrm{b}(t) + kz_\mathrm{b}(t) + (m_\mathrm{b}+m_\mathrm{w})g \\ = z_0([c\{\omega(t) + \dot{\omega}(t)t\} \\ + m_\mathrm{w}\{2\dot{\omega}(t) \\ + \ddot{\omega}(t)t\}]\cos(\omega(t)t) \\ + [k \\ - m_\mathrm{w}\{\omega(t) \\ + \dot{\omega}(t)t\}^2]\sin(\omega(t)t)) + \bar{F}(t). \end{aligned} \tag{3}$$

Dividing (3) by m_b, defining damping ratio $\xi = \frac{c}{2m_\mathrm{b}\omega_\mathrm{n}}$ and natural frequency of the system $\omega_\mathrm{n} = \sqrt{\frac{k}{m_\mathrm{b}}}\left(\frac{\mathrm{rad}}{\mathrm{s}}\right)$, equation (3) could be rewritten as:

$$\begin{aligned} \ddot{z}_\mathrm{b}(t) + 2\xi\omega_\mathrm{n}\dot{z}_\mathrm{b}(t) + \omega_\mathrm{n}^2 z_\mathrm{b}(t) \\ = z_0([2\xi\omega_\mathrm{n}\{\omega(t) + \dot{\omega}(t)t\} \\ + \alpha\{2\dot{\omega}(t) + \ddot{\omega}(t)t\}]\cos(\omega(t)t) \\ + [\omega_\mathrm{n}^2 \\ - \alpha\{\omega(t) + \dot{\omega}(t)t\}^2]\sin(\omega(t)t)) \\ + F(t) - (1+\alpha)g, \end{aligned} \tag{4}$$

where $\alpha = \frac{m_\mathrm{w}}{m_\mathrm{b}}$ is the ratio of the mass of the wings to the base.

To simplify (4), the time-varying flapping frequency $\omega(t)$ is replaced by its steady-state value ω_ss which keeps the robot flying steadily at a constant height. Therefore, (4) is rewritten as:

$$\begin{aligned} \ddot{z}_\mathrm{b}(t) + 2\xi\omega_\mathrm{n}\dot{z}_\mathrm{b}(t) + \omega_\mathrm{n}^2 z_\mathrm{b}(t) \\ = z_0(2\xi\omega_\mathrm{n}\omega_\mathrm{ss}\cos\omega_\mathrm{ss}t \\ + [\omega_\mathrm{n}^2 - \alpha\omega_\mathrm{ss}^2]\sin\omega_\mathrm{ss}t) + F(t) \\ - (1+\alpha)g. \end{aligned} \tag{5}$$

The objective of this section is to find the displacement transmissibility ratio, therefore, the free vibration of dynamics (5) is considered by $F(t) = 0$, which means the robot flies steadily in the air with a constant flapping wing. A possible form of a *particular* solution to (5) is presented:

$$z_{\mathrm{b,p},1}(t) = C_1\cos(\omega_\mathrm{ss}t + \phi_1), \tag{6}$$

$$z_{\mathrm{b,p},2}(t) = C_2\sin(\omega_\mathrm{ss}t + \phi_2), \tag{7}$$

where C_1, C_2, ϕ_1 and ϕ_2 are unknown constants. Substituting (6) into (5) and mathematical manipulation result in:

$$\begin{aligned} C_1\left(\left[1 - \left(\frac{\omega_\mathrm{ss}}{\omega_\mathrm{n}}\right)^2\right]\cos\phi_1 - 2\xi\frac{\omega_\mathrm{ss}}{\omega_\mathrm{n}}\sin\phi_1\right) \\ = z_0 2\xi\frac{\omega_\mathrm{ss}}{\omega_\mathrm{n}}, \end{aligned} \tag{8}$$

$$\begin{aligned} C_1\left(-\left[1 - \left(\frac{\omega_\mathrm{ss}}{\omega_\mathrm{n}}\right)^2\right]\sin\phi_1 - 2\xi\frac{\omega_\mathrm{ss}}{\omega_\mathrm{n}}\cos\phi_1\right) \\ = z_0\left[1 - \alpha\left(\frac{\omega_\mathrm{ss}}{\omega_\mathrm{n}}\right)^2\right]. \end{aligned} \tag{9}$$

Solving (8) and (9) simultaneously provides the first set of unknown constants

$$C_1 = z_0\frac{(1-\alpha r^2)^2 + (2\xi r)^2}{\sqrt{\{(1-\alpha r^2)^2 + (2\xi r)^2\}\{(1-r^2)^2 + (2\xi r)^2\}}}, \tag{10}$$

$$\phi_1 = \cos^{-1}\frac{2r^3(1-\alpha)\xi}{\sqrt{\{(1-\alpha r^2)^2 + (2\xi r)^2\}\{(1-r^2)^2 + (2\xi r)^2\}}}, \tag{11}$$

in which $r = \frac{\omega_\mathrm{ss}}{\omega_\mathrm{n}}$ is frequency ratio.

Similarly, the substitution of (7) into (5) generates:

$$\begin{aligned} C_2\left(\left[1 - \left(\frac{\omega_\mathrm{ss}}{\omega_\mathrm{n}}\right)^2\right]\sin\phi_2 + 2\xi\frac{\omega_\mathrm{ss}}{\omega_\mathrm{n}}\cos\phi_2\right) \\ = z_0 2\xi\frac{\omega_\mathrm{ss}}{\omega_\mathrm{n}}, \end{aligned} \tag{12}$$

$$\begin{aligned} C_2\left(\left[1 - \left(\frac{\omega_\mathrm{ss}}{\omega_\mathrm{n}}\right)^2\right]\cos\phi_2 - 2\xi\frac{\omega_\mathrm{ss}}{\omega_\mathrm{n}}\sin\phi_2\right) \\ = z_0\left[1 - \alpha\left(\frac{\omega_\mathrm{ss}}{\omega_\mathrm{n}}\right)^2\right]. \end{aligned} \tag{13}$$

Solving (12) and (13) simultaneously, the second set of constant parameters is found:

$$C_2 = z_0\frac{1 + \alpha r^4 - r^2(1 + \alpha - 4\xi^2)}{\sqrt{\{(1-\alpha r^2)^2 + (2\xi r)^2\}\{(1-r^2)^2 + (2\xi r)^2\}}}, \tag{14}$$

$$\phi_2 = \cos^{-1}\frac{1 + \alpha r^4 - r^2(1 + \alpha - 4\xi^2)}{\sqrt{\{(1-\alpha r^2)^2 + (2\xi r)^2\}\{(1-r^2)^2 + (2\xi r)^2\}}}. \tag{15}$$

The preprint version of the article: S. R. Nekoo and A. Ollero, "Equivalent Vertical Dynamics of Flapping-Wing Flying Robot in Regulation Control: Displacement Transmissibility Ratio," 2023 International Conference on Unmanned Aircraft Systems (ICUAS), Warsaw, Poland, 2023, pp. 1301-1307, doi: 10.1109/ICUAS57906.2023.10156157.

Summation of (6) and (7) provides the particular solution to (5) as:

$$z_{\mathrm{b,p}}(t) = z_{\mathrm{b,p},1}(t) + z_{\mathrm{b,p},2}(t) = C_1\cos(\omega_{\mathrm{ss}}t + \phi_1) + C_2\sin(\omega_{\mathrm{ss}}t + \phi_2). \quad (16)$$

Expansion of (16) generates:

$$z_{\mathrm{b,p}}(t) = D_1\cos\omega_{\mathrm{ss}}t + D_2\sin\omega_{\mathrm{ss}}t, \quad (17)$$

where $D_1 = C_1\cos\phi_1 + C_2\sin\phi_2$ and $D_2 = C_2\cos\phi_2 - C_1\sin\phi_1$. To find one oscillatory term as a particular solution to the dynamic equation (5), equation (17) is rewritten as:

$$z_{\mathrm{b,p}}(t) = R\cos(\omega_{\mathrm{ss}}t - \phi_3), \quad (18)$$

where

$$R = \sqrt{D_1^2 + D_2^2} = \sqrt{(C_1\cos\phi_1 + C_2\sin\phi_2)^2 + (C_2\cos\phi_2 - C_1\sin\phi_1)^2},$$
$$\phi_3 = \operatorname{atan}\frac{D_2}{D_1} = \operatorname{atan}\frac{C_2\cos\phi_2 - C_1\sin\phi_1}{C_1\cos\phi_1 + C_2\sin\phi_2}.$$

The *local* displacement transmissibility ratio is defined as the maximum response magnitude to displacement magnitude in steady-state response [1]:

$$\mathrm{TR} = \max z_{\mathrm{b,p}}(t_{\mathrm{ss}})\,/z_0,$$

which in our case generates the following displacement transmissibility:

$$\mathrm{TR}(\alpha,\xi,r) = \frac{R|\cos(\omega_{\mathrm{ss}}t - \phi_3)|}{z_0} = \frac{\sqrt{(C_1\cos\phi_1 + C_2\sin\phi_2)^2 + (C_2\cos\phi_2 - C_1\sin\phi_1)^2}}{z_0}. \quad (19)$$

Substitution of ϕ_1 and ϕ_2 into (19) results in:

$$\mathrm{TR}(\alpha,\xi,r) = \frac{\sqrt{\left(\beta_1\sigma_1 + \beta_2\sqrt{\mu^2 - \sigma_2^2}\right)^2 + \left(\beta_2\sigma_2 - \beta_1\sqrt{\mu^2 - \sigma_1^2}\right)^2}}{\mu^2},$$

where

$$\sigma_1 = 2r^3(1-\alpha)\xi,$$
$$\sigma_2 = 1 + \alpha r^4 - r^2(1 + \alpha - 4\xi^2),$$
$$\mu = \sqrt{\{(1-\alpha r^2)^2 + (2\xi r)^2\}\{(1-r^2)^2 + (2\xi r)^2\}},$$
$$\beta_1 = (1-\alpha r^2)^2 + (2\xi r)^2,$$
$$\beta_2 = 1 + \alpha r^4 - r^2(1 + \alpha - 4\xi^2).$$

The behavior of $\mathrm{TR}(\alpha,\xi,r)$ is important in the design of an ornithopter and should be reduced through parameter optimization and proper selection of damping and stiffness constants.

IV. Numerical Analysis

The local displacement transmissibility ratio starts from 0 and changes drastically between $r = [0.5,1.5]$ and it depends on $\alpha = \frac{m_{\mathrm{w}}}{m_{\mathrm{b}}}$, the ratio of the mass of wings to the base. For a series of $\alpha = \{0,0.2,0.4,0.6,0.8,0.95\}$ variables, the TR has been evaluated, presented in Fig. 3. $\alpha = 0$ indicates that the mass of the wing is zero which is not realistic and $\alpha > 0.5$ shows the cases where the mass of wings is greater than *half of the mass of the body* which is not realistic and that is only presented in this section to demonstrate the behavior of the local displacement transmissibility in the total range of $\alpha = [0,1)$, see Fig. 3. The results show that for different mass ratio, the frequency ratio should not be set between the following range $0.5 < r < 1.5$ where the transmission ratio is high. The simulation results also reveal that a damping ratio greater than $\xi > 0.5$ reduces the transmission ratio. The displacement transmissibility index ought to be less than $\mathrm{TR} < 1$ to keep the excitation of the body less than the excitation of the moving base. Section V will present a case study to define the parameters of the flapping-wing robot based on a preferable transmission ratio.

V. Design of the Parameters of the Flapping-Wing Robot

In this section, based on some physical parameters of the flapping-wing robot, the available range of local displacement transmissibility ratio is found. Then a proper damping ratio and an actuation flapping frequency are determined to constrain the parameter selection $\{\omega(t), k, c\}$ within a safe and proper zone. The mass of the body and wings are defined by the design though this TR study could influence the distribution of weight m_{b} and m_{w} as well. The total weight of the E-Flap robot was reported $510(\mathrm{g})$ [18]. Measuring the weight of the wings $m_{\mathrm{w}} = 150(\mathrm{g})$ and the rest of the body $m_{\mathrm{b}} = 360(\mathrm{g})$, result in weight ratio $\alpha = 0.4167$. This value generates the TR response in term of frequency ratio in the range of $r = [0,2.5]$, in Fig. 4. The stiffness constant of the equivalent system (1) could be computed. The excitation of the wings due to flapping is transferred to the body of the robot through the carbon fiber tube of the wing. The tube acts like a clamped-free beam with equivalent stiffness constant:

$$k = \frac{3EI}{L^3}\left(\frac{\mathrm{N}}{\mathrm{m}}\right), \quad (20)$$

where $E = 65\times10^9\left(\frac{\mathrm{N}}{\mathrm{m}^2}\right)$ is the elastic modulus of carbon fiber, length of the wing is $a = 0.75(m)$, which defines $L = 0.25(\mathrm{m})$ as the distance between the CoM of the body and effective lift force on the wing (see Fig. 5), $I = 5.1051\times10^{-11}(\mathrm{m}^4)$ is the second moment of the cross-sectional area of the tube, with an inner diameter of 4 and an outer diameter of $6(\mathrm{mm})$. This ultimately results in $k = 637.115\left(\frac{\mathrm{N}}{\mathrm{m}}\right)$. Stiffness constant generates the natural frequency of the flapping robot as $\omega_{\mathrm{n}} = 42.0686\left(\frac{\mathrm{rad}}{\mathrm{s}}\right)$. The relevant values of transmissibility rations for different damping ratios reported in Table 1 for two critical points of $r = \sqrt{2}/2$ and $r = \sqrt{2}$.

The preprint version of the article: S. R. Nekoo and A. Ollero, "Equivalent Vertical Dynamics of Flapping-Wing Flying Robot in Regulation Control: Displacement Transmissibility Ratio," 2023 International Conference on Unmanned Aircraft Systems (ICUAS), Warsaw, Poland, 2023, pp. 1301-1307, doi: 10.1109/ICUAS57906.2023.10156157.

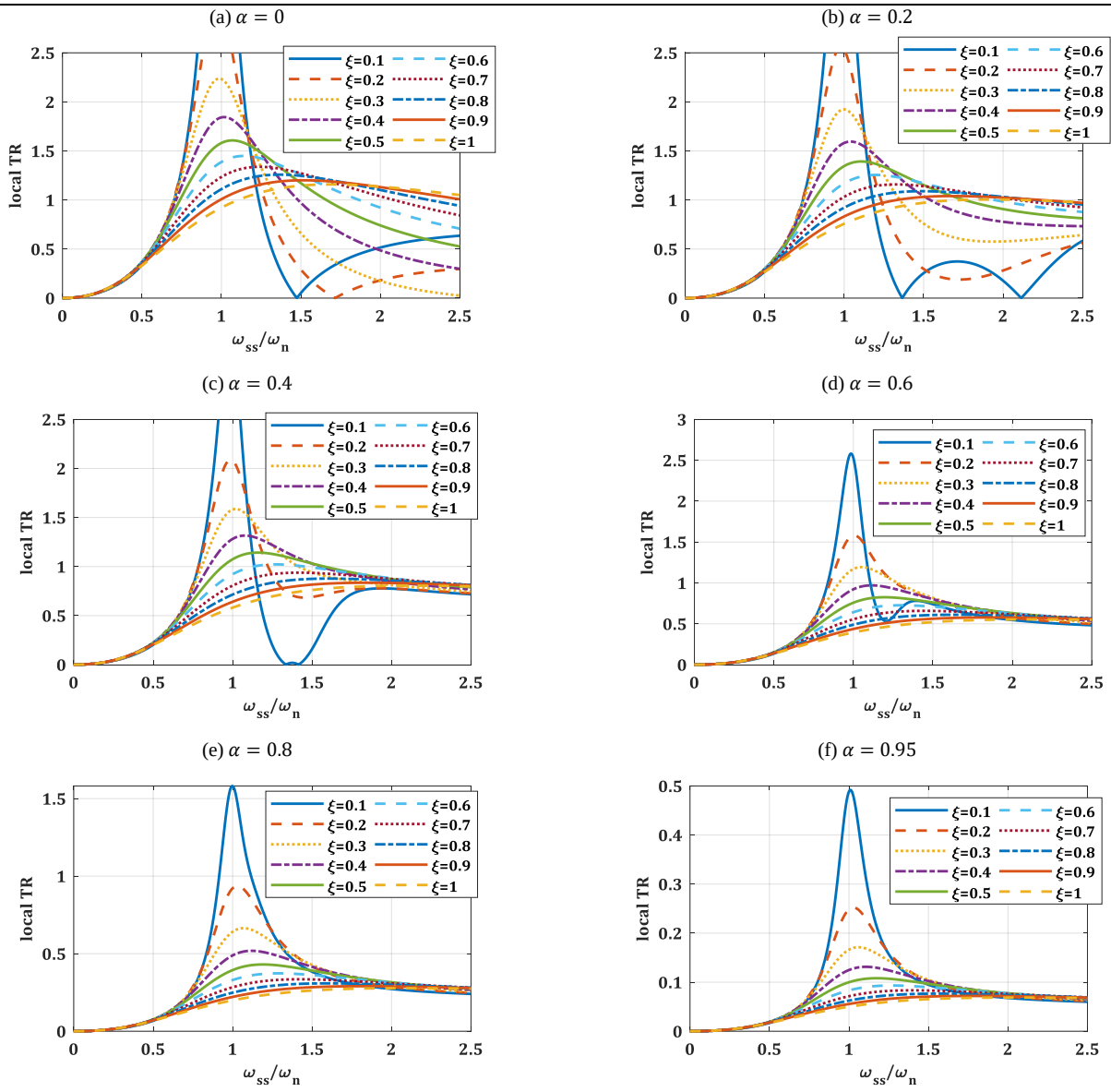

Fig. 3. The local displacement transmissibility for different values of $\alpha = \frac{m_w}{m_b}$ and damping ratio $\xi = [0.1, \ldots, 1]$, in $r = [0,2.5]$.

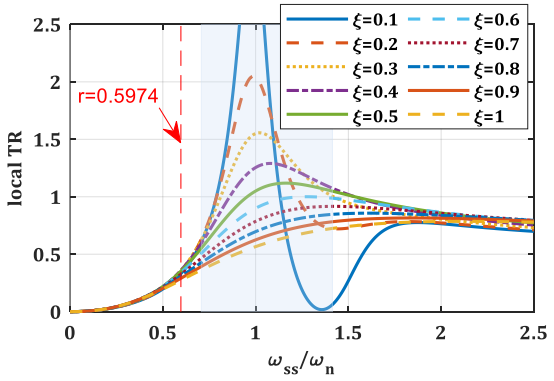

Fig. 4. The local displacement transmissibility for different values of $\alpha = 0.4286$ in $r = [0,2.5]$.

TABLE 1. THE TR RATIO AT $r = \frac{\sqrt{2}}{2}$ AND $r = \sqrt{2}$.

NO.	ξ	$r = \sqrt{2}/2$	$r = \sqrt{2}$
1	0.1	0.5971	0.0631
2	0.2	0.6227	0.7232
3	0.3	0.6182	1.0043
4	0.4	0.5883	1.0737
5	0.5	0.5468	1.0485
6	0.6	0.5032	0.9874
7	0.7	0.4617	0.9166
8	0.8	0.4241	0.8471
9	0.9	0.3906	0.7828
10	1	0.3611	0.7249

The preprint version of the article: S. R. Nekoo and A. Ollero, "Equivalent Vertical Dynamics of Flapping-Wing Flying Robot in Regulation Control: Displacement Transmissibility Ratio," 2023 International Conference on Unmanned Aircraft Systems (ICUAS), Warsaw, Poland, 2023, pp. 1301-1307, doi: 10.1109/ICUAS57906.2023.10156157.

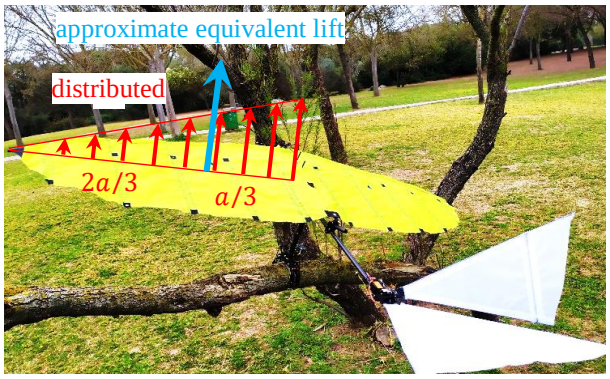

Fig. 5. The wing dimension and approximate value and position of the lift force.

The flapping frequency that provides approximately steady-state flight is $4(\mathrm{Hz})$ or $25.1327\left(\frac{\mathrm{rad}}{\mathrm{s}}\right)$. This value results in a frequency ratio $r = 0.5974$. Considering this frequency ratio and observing Fig. 4, the displacement transmissibility is in a good state for all damping ratio parameters, approximately around $\mathrm{TR} = 0.3$, varying between the range $[0.27, 0.36]$. The highest TR ratio is for $\xi = 0.7$ and the lowest one for $\xi = 1$.

VI. Conclusions

This work presented an investigation of the equivalent dynamic of the flapping flight in a vertically controlled motion. The data of the system for model creation was obtained from a series of real flight experiments in a testbed [8, 39]. The data was recorded by an Opti-Track motion capture system in a large indoor $20\mathrm{m} \times 15\mathrm{m} \times 7\mathrm{m}$ testbed with high accuracy with 28 cameras. The flight data constantly showed similar oscillatory behavior on the trajectories. This motivated us to find an equivalent system with similar behavior. The equivalent system enabled us to find an analytical expression for displacement transmissibility. If one could reduce the displacement transmissibility by the selection of the proper parameters, the oscillation would be reduced and the precision of the flight increases. This will help the control designer for better performance tuning and more success in perching on a branch which is an important phase of flight in FWFRs. This work presented the TR relation and it will be used for the parameter definition of the FWFR and reduction of that in future works.

Acknowledgment

This work was supported by the European Project GRIFFIN ERC Advanced Grant 2017, Action 788247; and HAERA (Spanish Ministry of Science and Innovation PID2020-119027RB-I00).

References

[1] S. G. Kelly, *Mechanical vibrations: theory and applications*: Cengage learning Stamford, USA, 2012.

[2] J. P. Den Hartog, *Mechanical vibrations*: Courier Corporation, 1985.

[3] W. Weaver Jr, S. P. Timoshenko, and D. H. Young, *Vibration problems in engineering*: John Wiley & Sons, 1991.

[4] F. Fahy and J. Walker, *Advanced applications in acoustics, noise and vibration*: CRC Press, 2018.

[5] A. Carrella, M. J. Brennan, T. P. Waters, and V. Lopes Jr, "Force and displacement transmissibility of a nonlinear isolator with high-static-low-dynamic-stiffness," *International Journal of Mechanical Sciences*, vol. 55, pp. 22-29, 2012.

[6] X. Wang, J. Zhou, D. Xu, H. Ouyang, and Y. Duan, "Force transmissibility of a two-stage vibration isolation system with quasi-zero stiffness," *Nonlinear Dynamics*, vol. 87, pp. 633-646, 2017.

[7] C. Cheng, S. Li, Y. Wang, and X. Jiang, "Force and displacement transmissibility of a quasi-zero stiffness vibration isolator with geometric nonlinear damping," *Nonlinear Dynamics*, vol. 87, pp. 2267-2279, 2017.

[8] R. Zufferey, J. T. Barbero, D. F. Talegon, S. R. Nekoo, J. A. Acosta, and A. Ollero, "How ornithopters can perch autonomously on a branch," *Nature Communications*, vol. 13, pp. 1-11, 2022.

[9] K. Ye and J. C. Ji, "An origami inspired quasi-zero stiffness vibration isolator using a novel truss-spring based stack Miura-ori structure," *Mechanical Systems and Signal Processing*, vol. 165, p. 108383, 2022.

[10] D.-D. Tan, Z.-Q. Lu, D.-H. Gu, H. Ding, and L.-Q. Chen, "A ring vibration isolator enhanced by a nonlinear energy sink," *Journal of Sound and Vibration*, vol. 508, p. 116201, 2021.

[11] K. Bodie, M. Brunner, M. Pantic, S. Walser, P. Pfändler, U. Angst, *et al.*, "Active interaction force control for contact-based inspection with a fully actuated aerial vehicle," *IEEE Transactions on Robotics*, vol. 37, pp. 709-722, 2020.

[12] S. Herkal, M. M. Rahman, S. Nagarajaiah, V. V. J. Harikrishnan, and P. Ajayan, "3D printed metamaterials for damping enhancement and vibration isolation: Schwarzites," *Mechanical Systems and Signal Processing*, vol. 185, p. 109819, 2023.

[13] J. Lee, S. Ryu, and H. J. Kim, "Stable flight of a flapping-wing micro air vehicle under wind disturbance," *IEEE Robotics and Automation Letters*, vol. 5, pp. 5685-5692, 2020.

[14] E. Pan, X. Liang, and W. Xu, "Development of vision stabilizing system for a large-scale flapping-wing robotic bird," *IEEE Sensors Journal*, vol. 20, pp. 8017-8028, 2020.

[15] X. Wu, W. He, Q. Wang, T. Meng, X. He, and Q. Fu, "A long-endurance flapping-wing robot based on mass distribution and energy consume method," *IEEE Transactions on Industrial Electronics*, 2022.

[16] H. Huang, W. He, J. Wang, L. Zhang, and Q. Fu, "An all servo-driven bird-like flapping-wing aerial robot capable of autonomous flight," *IEEE/ASME Transactions on Mechatronics*, vol. 27, pp. 5484-5494, 2022.

[17] A. Martín-Alcántara, P. Grau, R. Fernandez-Feria, and A. Ollero, "A simple model for gliding and low-amplitude flapping flight of a bio-inspired UAV," in *2019 International Conference on Unmanned Aircraft Systems (ICUAS)*, 2019, pp. 729-737.

[18] R. Zufferey, J. Tormo-Barbero, M. M. Guzmán, F. J. Maldonado, E. Sanchez-Laulhe, P. Grau, *et al.*, "Design of the high-payload flapping wing robot E-Flap," *IEEE*

The preprint version of the article: S. R. Nekoo and A. Ollero, "Equivalent Vertical Dynamics of Flapping-Wing Flying Robot in Regulation Control: Displacement Transmissibility Ratio," 2023 International Conference on Unmanned Aircraft Systems (ICUAS), Warsaw, Poland, 2023, pp. 1301-1307, doi: 10.1109/ICUAS57906.2023.10156157.

Robotics and Automation Letters, vol. 6, pp. 3097-3104, 2021.

[19] A. Chen, B. Song, Z. Wang, D. Xue, and K. Liu, "A novel actuation strategy for an agile bioinspired FWAV performing a morphing-coupled wingbeat pattern," *IEEE Transactions on Robotics*, 2022.

[20] S. R. Nekoo, J. Á. Acosta, and A. Ollero, "Combination of terminal sliding mode and finite-time state-dependent Riccati equation: Flapping-wing flying robot control," *Proceedings of the Institution of Mechanical Engineers, Part I: Journal of Systems and Control Engineering*, p. 09596518221138627, 2022.

[21] J. Mou, W. Zhang, K. Zheng, Y. Wang, and C. Wu, "More detailed disturbance measurement and active disturbance rejection altitude control for a flapping wing robot under internal and external disturbances," *Journal of Bionic Engineering*, vol. 19, pp. 1722-1735, 2022.

[22] H. Huang, W. He, J. Wang, L. Zhang, and Q. Fu, "An all servo-driven bird-like flapping-wing aerial robot capable of autonomous flight," *IEEE/ASME Transactions on Mechatronics*, 2022.

[23] Q. Li, A. Ji, H. Shen, R. Li, K. Liu, X. Zheng, *et al.*, "Experimental study on the wing parameter optimization of flapping-wing aircraft based on the clap-and-fling mechanism," *International Journal of Aeronautical and Space Sciences*, vol. 23, pp. 265-276, 2022.

[24] W. D. Shin, W. Stewart, M. A. Estrada, A. J. Ijspeert, and D. Floreano, "Elastic-actuation mechanism for repetitive hopping based on power modulation and cyclic trajectory generation," *IEEE Transactions on Robotics*, 2022.

[25] H. Gao, J. Hu, D. Liu, and J. Zhu, "Adaptive vibration control for two-stage bionic flapping wings based on neural network algorithm," in *2022 41st Chinese Control Conference (CCC)*, Hefei, China, 2022, pp. 3539-3544.

[26] A. Gómez Eguíluz, J. P. Rodríguez Gómez, R. Tapia, F. J. Maldonado, M.-d. D. R., J. A. Acosta, *et al.*, "Why fly blind? Event-based visual guidance for ornithopter robot flight," in *International Conference on Intelligent Robots and Systems (IROS 2021)*, Prague, Czech Republic, 2021.

[27] J. P. Rodríguez-Gómez, R. Tapia, M. M. G. Garcia, J. R. Martínez-de Dios, and A. Ollero, "Free as a bird: Event-based dynamic sense-and-avoid for ornithopter robot flight," *IEEE Robotics and Automation Letters*, vol. 7, pp. 5413-5420, 2022.

[28] J. P. Rodríguez-Gómez, R. Tapia, J. L. Paneque, P. Grau, A. G. Eguíluz, J. R. Martínez-de Dios, *et al.*, "The GRIFFIN perception dataset: Bridging the gap between flapping-wing flight and robotic perception," *IEEE Robotics and Automation Letters*, vol. 6, pp. 1066-1073, 2021.

[29] J. A. Moreno, C. Ruiz, A. Satué, J. Á. Acosta, and A. Ollero, "Design, development and testing of a Hybrid Fixed-Flapping wing UAV," in *2022 International Conference on Unmanned Aircraft Systems (ICUAS)*, 2022, pp. 329-338.

[30] W. Ding, Z. Liu, F. Zhang, L. Cui, and S. Wang, "Research on visual image processing and edge detection method of micro flapping wing flying robot based on cluster analysis," in *Seventh Asia Pacific Conference on Optics Manufacture and 2021 International Forum of Young Scientists on Advanced Optical Manufacturing (APCOM and YSAOM 2021)*, 2022, pp. 493-500.

[31] L. J. Roberts, H. A. Bruck, and S. K. Gupta, "Modeling of dive maneuvers in flapping wing unmanned aerial vehicles," in *2015 IEEE International Symposium on Safety, Security, and Rescue Robotics (SSRR)*, 2015, pp. 1-6.

[32] S. F. Armanini, M. Karásek, G. C. H. E. De Croon, and C. C. De Visser, "Onboard/offboard sensor fusion for high-fidelity flapping-wing robot flight data," *Journal of Guidance, Control, and Dynamics*, vol. 40, pp. 2121-2132, 2017.

[33] C. Ruiz, J. A. Acosta, and A. Ollero, "Aerodynamic reduced-order volterra model of an ornithopter under high-amplitude flapping," *Aerospace Science and Technology*, vol. 121, 2022.

[34] E. Sanchez-Laulhe, R. Fernandez-Feria, and A. Ollero, "Simplified model for forward-flight transitions of a bio-inspired unmanned aerial vehicle," *Aerospace*, vol. 9, p. 617, 2022.

[35] L. T. K. Au, H. V. Phan, S. H. Park, and H. C. Park, "Effect of corrugation on the aerodynamic performance of three-dimensional flapping wings," *Aerospace Science and Technology*, vol. 105, p. 106041, 2020.

[36] D. Bie, D. Li, J. Xiang, H. Li, Z. Kan, and Y. Sun, "Design, aerodynamic analysis and test flight of a bat-inspired tailless flapping wing unmanned aerial vehicle," *Aerospace Science and Technology*, vol. 112, p. 106557, 2021.

[37] C. T. Orlowski and A. R. Girard, "Dynamics, stability, and control analyses of flapping wing micro-air vehicles," *Progress in Aerospace Sciences*, vol. 51, pp. 18-30, 2012.

[38] Y. Xiaowu, S. Bifeng, Y. Wenqing, X. Dong, P. Yang, and L. Xinyu, "Study of aerodynamic and inertial forces of a dovelike flapping-wing MAV by combining experimental and numerical methods," *Chinese Journal of Aeronautics*, vol. 35, pp. 63-76, 2022.

[39] S. R. Nekoo, D. Feliu-Talegon, J. A. Acosta, and A. Ollero, "A 79.7 g manipulator prototype for E-Flap robot: A plucking-leaf application," *IEEE Access*, vol. 10, pp. 65300-65308, 2022.